

---

This is an electronic reprint of the original article.  
This reprint may differ from the original in pagination and typographic detail.

Author(s): Kokkonen, Kimmo & Kaivola, Matti & Benchabane, Sarah & Khelif, Abdelkrim & Laude, Vincent

Title: Scattering of surface acoustic waves by a phononic crystal revealed by heterodyne interferometry

Year: 2007

Version: Final published version

**Please cite the original version:**

Kokkonen, Kimmo & Kaivola, Matti & Benchabane, Sarah & Khelif, Abdelkrim & Laude, Vincent. 2007. Scattering of surface acoustic waves by a phononic crystal revealed by heterodyne interferometry. *Applied Physics Letters*. Volume 91, Issue 8. ISSN 0003-6951 (printed). DOI: 10.1063/1.2768910.

Rights: © 2007 American Institute of Physics (AIP). This article may be downloaded for personal use only. Any other use requires prior permission of the author and the American Institute of Physics.  
<http://scitation.aip.org/content/aip/journal/apl>

---

All material supplied via Aaltodoc is protected by copyright and other intellectual property rights, and duplication or sale of all or part of any of the repository collections is not permitted, except that material may be duplicated by you for your research use or educational purposes in electronic or print form. You must obtain permission for any other use. Electronic or print copies may not be offered, whether for sale or otherwise to anyone who is not an authorised user.

## Scattering of surface acoustic waves by a phononic crystal revealed by heterodyne interferometry

Kimmo Kokkonen, Matti Kaivola, Sarah Benchabane, Abdelkrim Khelif, and Vincent Laude

Citation: [Applied Physics Letters](#) **91**, 083517 (2007); doi: 10.1063/1.2768910

View online: <http://dx.doi.org/10.1063/1.2768910>

View Table of Contents: <http://scitation.aip.org/content/aip/journal/apl/91/8?ver=pdfcov>

Published by the [AIP Publishing](#)

---

### Articles you may be interested in

[Local resonances in phononic crystals and in random arrangements of pillars on a surface](#)

J. Appl. Phys. **114**, 104503 (2013); 10.1063/1.4820928

[Analysis of surface acoustic wave propagation in a two-dimensional phononic crystal](#)

J. Appl. Phys. **112**, 023524 (2012); 10.1063/1.4740050

[Surface acoustic wave band gaps in a diamond-based two-dimensional locally resonant phononic crystal for high frequency applications](#)

J. Appl. Phys. **111**, 014504 (2012); 10.1063/1.3673874

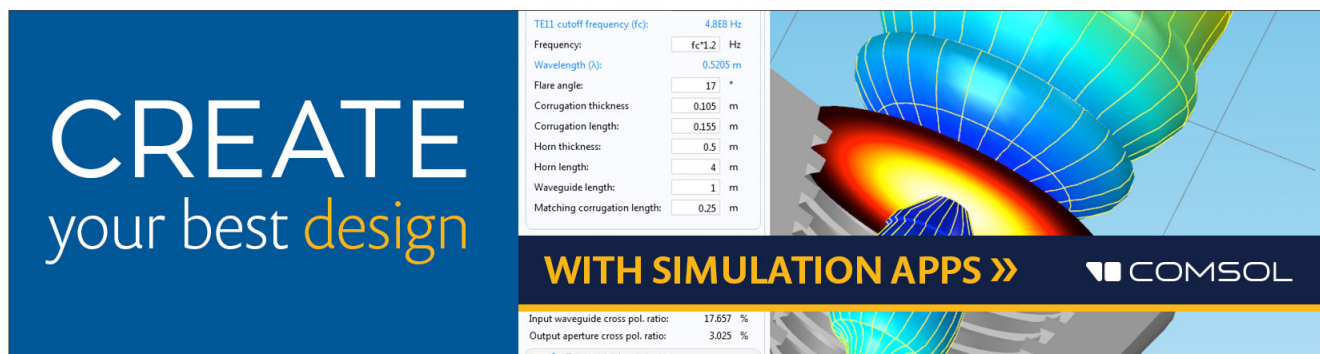
[Observation of surface-guided waves in holey hypersonic phononic crystal](#)

Appl. Phys. Lett. **98**, 171908 (2011); 10.1063/1.3583982

[Propagation of acoustic waves and waveguiding in a two-dimensional locally resonant phononic crystal plate](#)

Appl. Phys. Lett. **97**, 193503 (2010); 10.1063/1.3513218

---

An advertisement for COMSOL simulation software. On the left, a blue box contains the text 'CREATE your best design' in white and yellow. In the center, a white box lists simulation parameters for a TE11 cutoff frequency: Frequency (fc) = 4.868 Hz, Wavelength (lambda) = 0.5205 m, Flare angle = 17 degrees, Corrugation thickness = 0.105 m, Corrugation length = 0.155 m, Horn thickness = 0.5 m, Horn length = 4 m, Waveguide length = 1 m, and Matching corrugation length = 0.25 m. Below this, a table shows 'Input waveguide cross pol. ratio: 17.657 %' and 'Output aperture cross pol. ratio: 3.025 %', with a checkmark indicating 'Target criterion: passed'. On the right, a 3D simulation image shows a horn-shaped waveguide structure with a color-coded field distribution. The COMSOL logo is in the bottom right corner.

TE11 cutoff frequency (fc):	4.868 Hz
Frequency:	fc*1.2 Hz
Wavelength (lambda):	0.5205 m
Flare angle:	17 degrees
Corrugation thickness:	0.105 m
Corrugation length:	0.155 m
Horn thickness:	0.5 m
Horn length:	4 m
Waveguide length:	1 m
Matching corrugation length:	0.25 m

Input waveguide cross pol. ratio:	17.657 %
Output aperture cross pol. ratio:	3.025 %
Target criterion:	passed

## Scattering of surface acoustic waves by a phononic crystal revealed by heterodyne interferometry

Kimmo Kokkonen<sup>a)</sup> and Matti Kaivola

*Optics and Molecular Materials Laboratory, Helsinki University of Technology, P.O. Box 3500, FI-02015, TKK, Finland*

Sarah Benchabane, Abdelkrim Khelif, and Vincent Laude

*Institut FEMTO-ST, CNRS UMR 6174, Université de Franche-Comté, 32 Avenue de l'Observatoire, 25044 Besançon Cedex, France*

(Received 27 June 2007; accepted 16 July 2007; published online 24 August 2007)

Surface acoustic wave propagation within a two-dimensional phononic band gap structure has been studied using a heterodyne laser interferometer. Acoustic waves are launched by interdigital transducers towards a square lattice of holes etched in a piezoelectric medium. Interferometer measurements performed at frequencies lying below, within, and above the expected band gap frequency range provide direct information of the wave interaction with the phononic crystal, revealing anisotropic scattering into higher diffraction orders depending on the apparent grating pitch at the boundary between the phononic crystal and free surface. Furthermore, the measurements also confirm the existence of an elastic band gap, in accordance with previous electrical measurements and theoretical predictions. © 2007 American Institute of Physics.

[DOI: [10.1063/1.2768910](https://doi.org/10.1063/1.2768910)]

Phononic crystals (PCs) are two- or three-dimensional periodic structures that consist of two materials with different elastic constants, giving rise to absolute stop bands for acoustic wave propagation in the material.<sup>1,2</sup> They offer interesting new possibilities to engineer sophisticated transfer functions for microacoustic components. Recently, elastic stop bands for surface acoustic waves (SAWs) have been at the center of a growing research effort.<sup>3-7</sup> Experimental demonstrations of directional<sup>8</sup> as well as full band gaps<sup>9</sup> in piezoelectric crystals at the micrometer scale have been reported. These studies have taken advantage of the possibility to directly generate and receive SAWs by using interdigital transducers (IDTs),<sup>10</sup> thus allowing testing of PCs in realistic device configurations via electrical measurements. This characterization method, however, yields only indirect information on the wave interaction with the PC. In contrast, optical imaging of SAWs on the crystal surface is expected to reveal direct information on scattering and diffraction of waves in such anisotropic structures. In Refs. 11 and 12, laser generation and detection of ultrasound was used to obtain the dispersion of SAWs in one- and two-dimensional PCs. Another technique for probing SAW fields is scanning laser interferometry (see, e.g., Refs. 13 and 14 for recent accounts of the method). This technique is especially suited to characterizing SAWs electrically generated by standard IDTs on a piezoelectric substrate.

In this letter, a scanning heterodyne laser interferometer has been used to directly image the actual acoustic wave fields within a PC SAW device. The interferometric measurements have been performed below, within, and above the theoretically predicted and electrically confirmed forbidden frequency range. Besides confirming the existence of a band gap, the measurements reveal the existence of anisotropic scattering, as well as provide direct observation of higher order diffraction above the band gap.

The samples were fabricated onto standard 500  $\mu\text{m}$  thick *Y*-cut  $\text{LiNbO}_3$  substrates and they feature a PC in a delay line configuration similar to that presented in Ref. 9. The PC structure between the two IDTs is composed of a square lattice of 10  $\mu\text{m}$  deep holes with a diameter of 9.4  $\mu\text{m}$  and a pitch of 10  $\mu\text{m}$ . According to finite element simulations,<sup>9</sup> the resulting filling fraction of 69% theoretically ensures a full band gap for SAWs in a frequency range between 175 and 230 MHz. The actual full band gap was determined through electrical characterization of the devices and was found to extend from 200 up to 230 MHz. The difference between the predicted and experimental full band gap widths is attributed to the conicity of the holes.<sup>9</sup>

Direct optical measurements of the SAW fields in the PC devices for the  $\Gamma M$  direction were carried out with the scanning heterodyne laser interferometer presented in Ref. 14, featuring phase-sensitive absolute-amplitude detection of the SAW field at each measurement point. A set of three devices operating, respectively, below, within, and above the band gap was selected, with center frequencies of 176, 206, and 260 MHz, and a 12% fractional bandwidth for each of them.

In order to study the device behavior, large area scans, consisting of an area of  $650 \times 600 \mu\text{m}^2$ , were measured over the whole delay line structure with a lateral scanning step of 2.1  $\mu\text{m}$ . The amplitude fields at three selected frequencies are presented on the first row of Fig. 1. More detailed measurements of the wave interaction with the PC are provided on the second to fourth rows of Fig. 1. In these measurements, only the center of the acoustic beam, including the space in between the two IDTs, corresponding to an area of  $205 \times 205 \mu\text{m}^2$ , is scanned with a lateral scanning step smaller than 1  $\mu\text{m}$ . The scanning step was chosen to be small enough to also facilitate probing of the wave field in between the etch holes. The amplitude data have been averaged in the *y* direction at each frequency to provide an averaged line profile of the wave amplitude along the propagation path (see the third row of Fig. 1).

<sup>a)</sup>Electronic mail: kimmo.kokkonen@tkk.fi

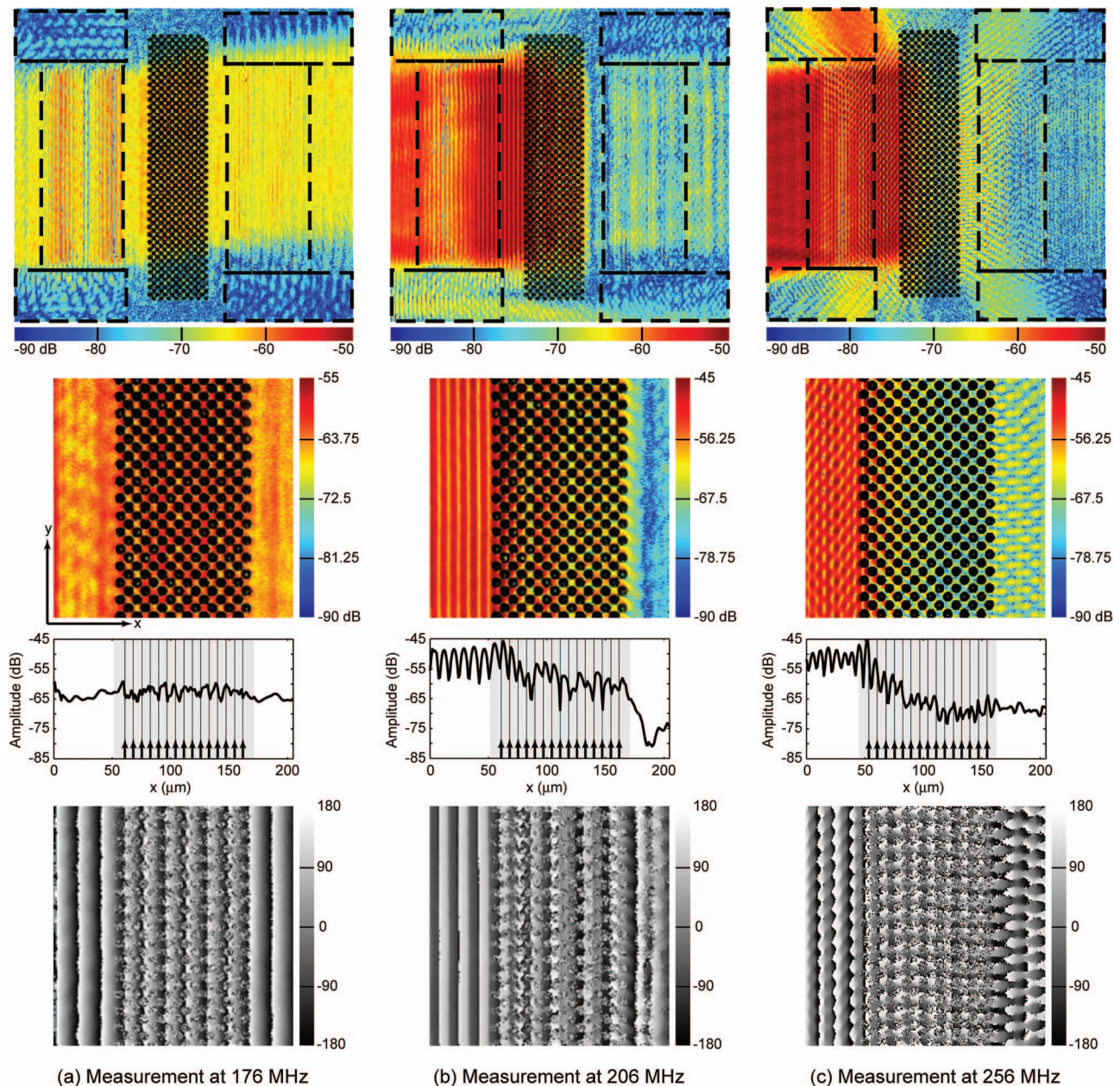


FIG. 1. (Color) Measured wave fields for the same phononic crystal structure with IDTs operating (a) below the band gap, at 176 MHz (b) within the band gap, at 206 MHz, and (c) above the band gap, at 256 MHz. The acoustic band gap exists for frequencies between 200 and 230 MHz. In each case, the left hand side IDT is emitting while the right hand side IDT is receiving. The first row shows large area scans with the PC structure overlaid on the amplitude image. The locations of the IDTs and their busbars are indicated with dashed black lines. More detailed scans of the amplitude and phase of the wave field are presented in rows 2 and 4, respectively. The PC structure is overlaid on the amplitude images to indicate the locations of the holes. The amplitude data of row two are averaged in the  $y$  direction and the resulting line profiles of the averaged amplitude along the wave propagation direction ( $x$ ) are presented as graphs in the third row. The location of the PC structure is marked with gray area. Due to the PC geometry, filling fraction, and scan step used, there are  $x$ -coordinate values at which only few good data points are available for the averaging. These locations are marked on the graphs by arrows and lines.

At frequencies below the onset frequency of the band gap (at 200 MHz), the SAWs pass through the PC lattice with relatively undisturbed phase fronts, revealing that the wave motion corresponds to a fairly pure traveling wave [see Fig. 1(a)]. Furthermore, no significant reflection, scattering, or other losses are observed, indicating that the PC does not significantly interfere with the wave motion. The beam steering angle due to the anisotropy of SAW propagation on lithium niobate is clearly observed and is in accordance with the theoretical value of  $6^\circ$  for the direction considered.

When operating at a frequency within the band gap, the PC structure is very reflective, resulting in a strong standing wave pattern seen on the left side of the PC in Fig. 1(b).

between the transmitting IDT and the PC. This behavior is accompanied by a low transmission leading nearly to an absence of wave amplitude on the other side of the PC structure. The phase fronts of the wave field, however, remain relatively undisturbed. These measurements thus confirm the existence of the predicted band gap along the  $\Gamma M$  propagation direction.<sup>9</sup>

Above the acoustic band gap, good transmission of SAWs is expected. However, the PC is observed to scatter the wave field at angles different from normal incidence, which results in a lobe structure visible both in the measured amplitude and phase fields [see Fig. 1(c)]. Despite the scattering, the PC does not cause a significant attenuation to

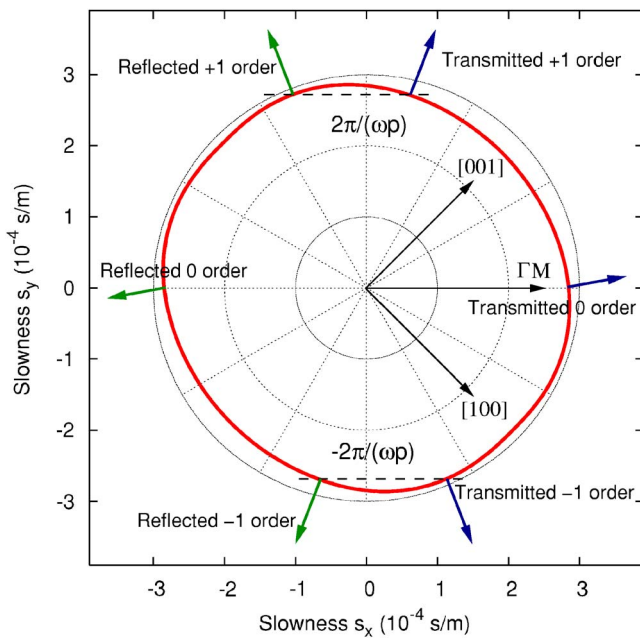


FIG. 2. (Color online) Construction of diffraction orders on both sides of the phononic crystal from the slowness curve for SAW on the free surface of lithium niobate.  $p = \sqrt{2}a$  is the apparent grating pitch. The frequency  $\omega/2\pi = 256$  MHz is used for the construction of diffraction orders shown. Below 248 MHz all diffraction orders except the zeroth are evanescent. The direction of the Poynting vector for diffraction orders corresponding to propagating waves is indicated by an arrow.

the wave field as within the band gap. The observed scattering can be explained by noting that, above a certain threshold frequency, the PC acts as an anisotropic diffraction grating. The apparent grating pitch is  $p = \sqrt{2}a$  in the  $\Gamma M$  direction considered here. The evanescent or propagative nature of the diffraction orders can be obtained from the slowness curve construction of Fig. 2, by requesting that the wave vector along the boundary between the PC and the free surface is  $k_y = 2\pi n/p$  for the  $n$ th diffraction order. Diffraction appears when the wave vector component along  $y$  of the first order satisfies  $k_y = 2\pi/p < \omega s$ , where  $s$  is the slowness in the  $y$  direction. This gives a threshold frequency of 248 MHz, which lies below the frequency of 256 MHz of the measurement data presented in Fig. 1(c). In comparison, the threshold frequency for the appearance of diffraction for the  $\Gamma X$  or

$\Gamma Y$  directions would be approximately 350 MHz, because in this case the grating pitch is smaller ( $p = a$ ). As a side effect of diffraction, we note that for efficient reception of the wave at the receiving IDT, the phase fronts of the wave should match the finger geometry of the IDT. Therefore it is to be expected that if the phase fronts of the transmitted wave are distorted due to, e.g., scattering, electrical measurements will likely result in a low value of transmission.

In conclusion, the surface-acoustic wave fields within a two-dimensional phononic crystal structure have been imaged in amplitude and phase by the use of a scanning heterodyne interferometer. These measurements confirm the existence of a band gap for surface acoustic waves previously predicted theoretically and via electrical measurements. They reveal that SAWs are transmitted almost unaffected below the band gap and strongly reflected within it. Above the band gap, scattering to higher diffraction orders appears depending on the apparent grating pitch as seen at the boundary between the PC and the free surface. These results open up interesting prospects for probing more complex spatial geometries such as elastic waveguides, defect modes, and diffractive structures managed in phononic crystals.

K.K. thanks the Finnish Cultural Foundation and Nokia Foundation for Scholarships.

- <sup>1</sup>M. S. Kushwaha, P. Halevi, L. Dobrzynski, and B. Djafari-Rouhani, Phys. Rev. Lett. **71**, 2022 (1993).
- <sup>2</sup>M. Sigalas and E. N. Economou, Solid State Commun. **86**, 141 (1993).
- <sup>3</sup>T. Aono and S.-I. Tamura, Phys. Rev. B **58**, 4838 (1998).
- <sup>4</sup>Y. Tanaka and S. I. Tamura, Phys. Rev. B **60**, 13294 (1999).
- <sup>5</sup>M. Torres, F. R. Montero de Espinosa, D. García-Pablos, and N. García, Phys. Rev. Lett. **82**, 3054 (1999).
- <sup>6</sup>T. Wu, Z. Huang, and S. Lin, Phys. Rev. B **69**, 094301 (2004).
- <sup>7</sup>V. Laude, M. Wilm, S. Benchabane, and A. Khelif, Phys. Rev. E **71**, 036607 (2005).
- <sup>8</sup>T. Wu, L. Wu, and Z. Huang, J. Appl. Phys. **97**, 094916 (2005).
- <sup>9</sup>S. Benchabane, A. Khelif, J.-Y. Rauch, L. Robert, and V. Laude, Phys. Rev. E **73**, 065601(R) (2006).
- <sup>10</sup>R. M. White and F. W. Voltmer, Appl. Phys. Lett. **17**, 314 (1965).
- <sup>11</sup>L. Dhar and J. A. Rogers, Appl. Phys. Lett. **77**, 1402 (2000).
- <sup>12</sup>D. M. Profunser, O. B. Wright, and O. Matsuda, Phys. Rev. Lett. **97**, 055502 (2006).
- <sup>13</sup>J. V. Knuutila, P. T. Tikka, and M. M. Salomaa, Opt. Lett. **25**, 613 (2000).
- <sup>14</sup>K. Kokkonen, J. V. Knuutila, V. P. Plessky, and M. M. Salomaa, Proc.-IEEE Ultrason. Symp. **2**, 1145 (2003).